

Crystal engineering in the *gem*-alkynol family; synthon repetitivity and topological similarity in diphenylethynylmethanols: structures that lack O—H···O hydrogen bonds

Clair Bilton,^a Judith A. K. Howard,^a N. N. L. Madhavi,^b Ashwini Nangia,^b Gautam R. Desiraju,^b Frank H. Allen^{c*} and Chick C. Wilson^d

^aDepartment of Chemistry, University of Durham, South Road, Durham DH1 3LE, England, ^bSchool of Chemistry, University of Hyderabad, Hyderabad 500 046, India, ^cCambridge Crystallographic Data Centre, 12 Union Road, Cambridge CB2 1EZ, England, and ^dISIS Facility, Rutherford Appleton Laboratory, Chilton, Didcot, Oxon OX11 0QX, England

Correspondence e-mail: allen@ccdc.cam.ac.uk

The structures of four *para*-substituted derivatives of diphenylethynylmethanol have been determined [ditolyethynylmethanol, di(4-chlorophenyl)ethynylmethanol, di(4-bromophenyl)ethynylmethanol and bis(4,4'-biphenyl)ethynylmethanol]. The dimethyl, dichloro, dibromo and diphenyl compounds have been analysed using X-ray diffraction at 150 K, and the dichloro compound has also been studied using neutron diffraction at 150 K. In common with the parent diphenylethynylmethanol [Garcia, Ramos, Rodriguez & Fronczek (1995). *Acta Cryst. C* **51**, 2674–2676], all four derivatives fail to form the expected strong O—H···O hydrogen bonds due to steric hindrance. Instead, the supramolecular structural organization in this family of *gem*-alkynols is mediated by a variety of weaker interactions. The two most acidic protons, O—H and C≡C—H, participate in weak hydrogen bonds to π -acceptors, forming synthons that stabilize all five structures. These primary interactions are reinforced by a variety of other weak hydrogen bonds involving C—H donors and the hydroxy-O as an acceptor, and by halogen···halogen interactions in the dichloro and dibromo compounds.

Received 31 May 2000
Accepted 22 August 2000

1. Introduction

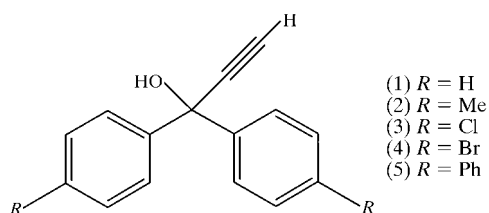
The identification of robust and reproducible supramolecular synthons (Desiraju, 1995) is a major goal of crystal engineering studies. The aim is to understand these patterns in terms of the mutual interplay between particular interactions (Nangia & Desiraju, 1998; Desiraju, 1997) and to establish correspondences between molecular and crystal structures (see *e.g.* Ermer & Eling, 1994; Allen *et al.*, 1997).

Previous papers (Bilton *et al.*, 1999; Madhavi, Bilton *et al.*, 2000; Madhavi, Desiraju *et al.*, 2000), have discussed the wide variety of interaction patterns observed in existing structures in the *gem*-alkynol family and reported nine crystal structures of seven novel compounds containing the 1,4-bis(*gem*-alkynol) functionality attached to cyclohexane and cyclohexa-2,5-diene rings. In all cases, the dominant synthon is constructed from strong cooperative arrangements of O—H···O hydrogen bonds which form extended chains, helical trimers, or cyclic tetramers and hexamers.

During our literature surveys, conducted using the Cambridge Structural Database (CSD; Allen & Kennard, 1993), we became intrigued by the structure of diphenylethynylmethanol [(1), $P2_1/n$, $Z = 4$; Garcia *et al.*, 1995]. Here (Fig. 1), inversion-related molecules form dimeric synthons through O—H··· π (arene) bonds and these dimers are linked by cooperative chains of C≡C—H··· π (ethynyl) bonds. The

structure is stabilized entirely by weak interactions: the O—H···O hydrogen bonds that might be expected by consideration of Etter's (1990) rule and from our own previous work in this series simply do not form.

Since there is considerable current interest in weak interactions (see Desiraju & Steiner, 1999), and because of our ongoing work on *gem*-alkynols, we decided to synthesize and study the structures of other members of the diphenylethynylmethanol family. The hope was to add to the growing literature describing O—H··· π (Steinwender *et al.*, 1993; Steiner, Starikov & Tamm, 1996) and C—H··· π interactions (Steiner *et al.*, 1995; Steiner, Tamm *et al.*, 1996; Lutz *et al.*, 1998; Nishio *et al.*, 1998). In this paper we report the structures of simple derivatives of (1), which are *para*-disubstituted by methyl (2), chloro (3), bromo (4) and phenyl (5) groups. Low-temperature X-ray diffraction has been used throughout and for (3) a low-temperature neutron diffraction experiment was also performed.



2. Experimental

2.1. Syntheses

Compounds (2)–(5) were synthesized from appropriately substituted dibenzophenone derivatives using a two-step procedure. All operations were carried out in a dry nitrogen atmosphere using standard syringe-septum techniques.

(i) A solution of trimethylsilylacetylene (4.4 mmol) in thf (15 ml) was mixed with *n*-butyllithium (4.2 mmol) at 195 K. After stirring for 15 min a solution of the substituted dibenzophenone was added dropwise and stirring was continued for 30 min at 195 K and for a further 1 h at room temperature. Brine was added to the reaction mixture and the products were extracted with diethylether. The organic phase was dried over magnesium sulfate, filtered and the ether removed.

(ii) The solid product from step (i) was dissolved in methanol and methanolic KOH was added slowly and stirred for 1 h at room temperature. The product was dried over magnesium sulfate and the solvent removed. Crystals were obtained by purification of the crude material (column chromatography) followed by recrystallization.

Melting points: (2) 368–369, (3) 345–346, (4) 370 and (5) 430 K. Spectroscopic data have been deposited.¹

2.2. Crystal structure analyses

X-ray diffraction intensities for (2)–(5) were collected at 150 K (Oxford Cryosystems cryostat) on a Bruker SMART

CCD diffractometer (Bruker Systems Inc., 1999a) using Mo $K\alpha$ X-radiation. Data were processed using the *SAINTE* package (Bruker Systems Inc., 1999b), with structure solution and refinement using *SHELX97* (Sheldrick, 1997). H atoms were located in all four structures and refined freely with isotropic displacement parameters. A large ($2.5 \times 1.5 \times 0.5$ mm³) crystal of (3) was selected for neutron diffraction study. Diffraction data were collected at 150 K on the SXD diffractometer (Keen & Wilson, 1996) at the ISIS spallation source, Rutherford Appleton Laboratory, Chilton, England. Data were processed using *SXD97* (Wilson, 1997), and coordinates for C and O atoms from the X-ray refinement were used as a starting model for least-squares refinement against the neutron data. H atoms were located from the resulting difference map and included in the neutron refinement model. Crystal data and details of data collections, structure solutions and refinements are given in Table 1. Atomic coordinates for non-H atoms are given in Table 2.

3. Results and discussion

Crystal structures of (1) (Garcia *et al.*, 1995) and (2), (3), (4) and (5) (this work) are illustrated in Figs. 1–5, while Fig. 6 provides schematic drawings of the synthons observed in these structures. Geometrical details of the intermolecular interactions observed in (2)–(5) are collected in Table 3.

3.1. Diphenylethynylmethanol (1) (Garcia *et al.*, 1995)

Inversion-related dimers (synthon I, Fig. 6) are formed through O—H··· π (arene) interactions, with herringbone

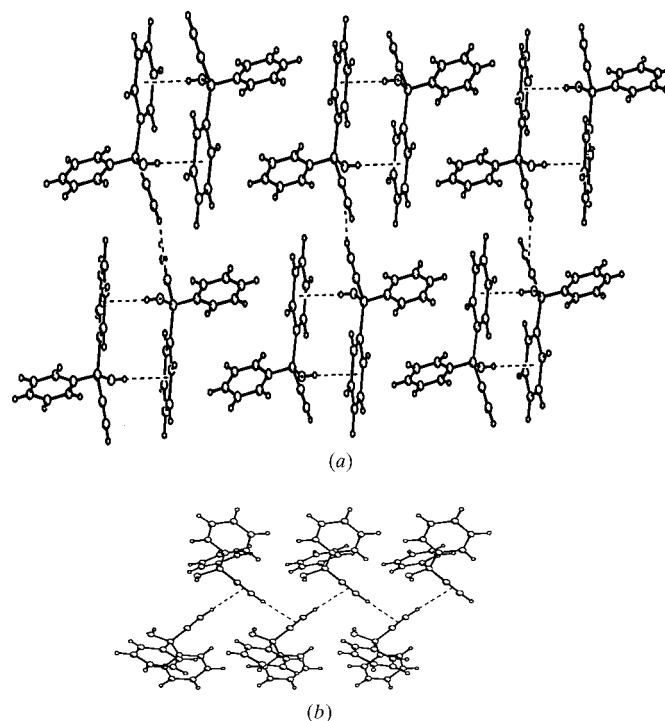


Figure 1
Perspective views of structure (1), displaying synthon I and other interactions.

¹Supplementary data for this paper are available from the IUCr electronic archives (Reference: BM0034). Services for accessing these data are described at the back of the journal.

interactions mediating the packing of dimers (Fig. 1*a*). The ethynyl groups project outwards from the two-dimensional arrangement of dimers, and form cooperative chains of $\text{C}\equiv\text{C}-\text{H}\cdots\pi(\text{ethynyl})$ bonds along the *b* axis (Fig. 1*b*).

3.2. Ditolyethynylmethanol (2)

The most notable similarity between the structures of parent (1) and the dimethyl derivative (2) is the lack of $\text{O}-\text{H}\cdots\text{O}$ hydrogen bonding: molecules of (2) form inversion-related $\text{O}-\text{H}\cdots\pi(\text{arene})$ dimers (Fig. 2*a*) as in (1). However, there is a different mutual arrangement of dimers in (2), where the two-dimensional packing is now mediated by a variety of weak interactions involving methyl $\text{C}-\text{H}$ donor groups and $\pi(\text{arene})$, $\pi(\text{ethynyl})$ and hydroxy-O acceptors. Thus, synthon I (Fig. 6) is preserved in structure (2). This synthon is also observed in the very closely related structure of 1,1,2-triphenylethanol (Ferguson *et al.*, 1994).

The ethynyl groups again project outwards from the two-dimensional arrangement of dimers but, in contrast to (1), these groups now form $\text{C}\equiv\text{C}-\text{H}\cdots\pi(\text{arene})$ interactions which link the molecules along the *b* axis to form synthon IV (Fig. 6). This difference in the involvement of the ethynyl group in structure (2) may be attributed to the bulky methyl groups, which disturb the structural arrangement adopted for the parent (1), but not sufficiently to prevent formation of the $\text{O}-\text{H}\cdots\pi(\text{arene})$ dimer.

3.3. Di(4-chlorophenyl)ethynylmethanol (3) and di(4-bromophenyl)ethynylmethanol (4)

Compounds (3) and (4) are isostructural, a not unexpected outcome (Pedireddi *et al.*, 1992), and are again characterized

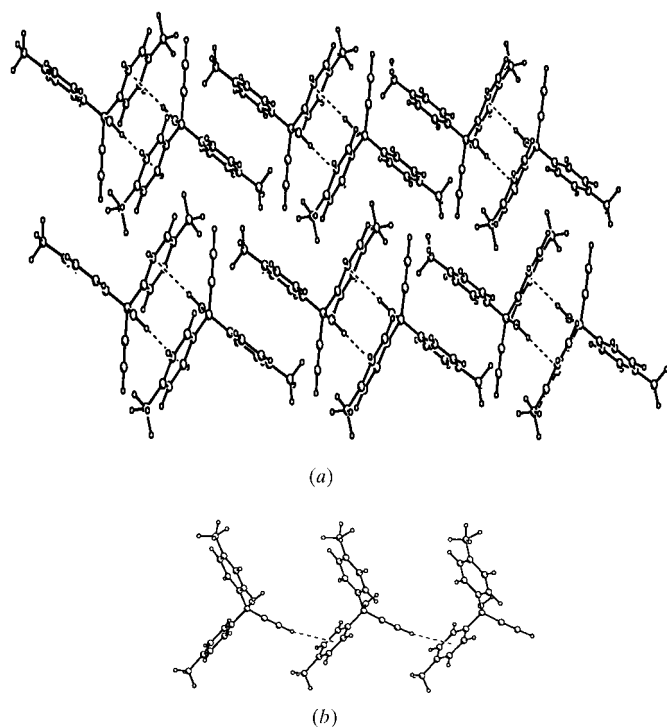


Figure 2
Perspective views of structure (2), displaying synthons I and IV.

by a lack of $\text{O}-\text{H}\cdots\text{O}$ hydrogen bonding. Figs. 3(*a*) and 4(*a*) show that both structures form dimers through $\text{C}\equiv\text{C}-\text{H}\cdots\pi(\text{arene})$ interactions to form synthon II of Fig. 6. Each constituent molecule of this synthon is then further dimerized *via* a pair of weaker $\text{C}(\text{phenyl})-\text{H}\cdots\text{O}$ interactions to form stacks along the *b* axis. The molecular stacks of (3) and (4) are linked along the *a* axis (Figs. 3*b* and 4*b*) by $\text{O}-\text{H}\cdots\pi(\text{arene})$ interactions, depicted as synthon III in Fig. 6, a situation which is further assisted by the weaker $\text{C}(\text{phenyl})-\text{H}\cdots\pi(\text{ethynyl})$ interactions.

Figs. 3(*a*), (*b*), 4(*a*) and (*b*) also show that the molecular stacks of (3) and (4) are cross-linked along the *c* axis by halogen \cdots halogen interactions. Recent debate concerning the nature and origin of these interactions is surveyed and illustrated in our previous paper (Madhavi, Desiraju *et al.*, 2000). In summary, intermolecular perturbation theory calculations (Price *et al.*, 1994; Lommerse *et al.*, 1996) show that carbon-bound halogens in a sufficiently electron-withdrawing environment present an anisotropic charge distribution, δ^+ forward

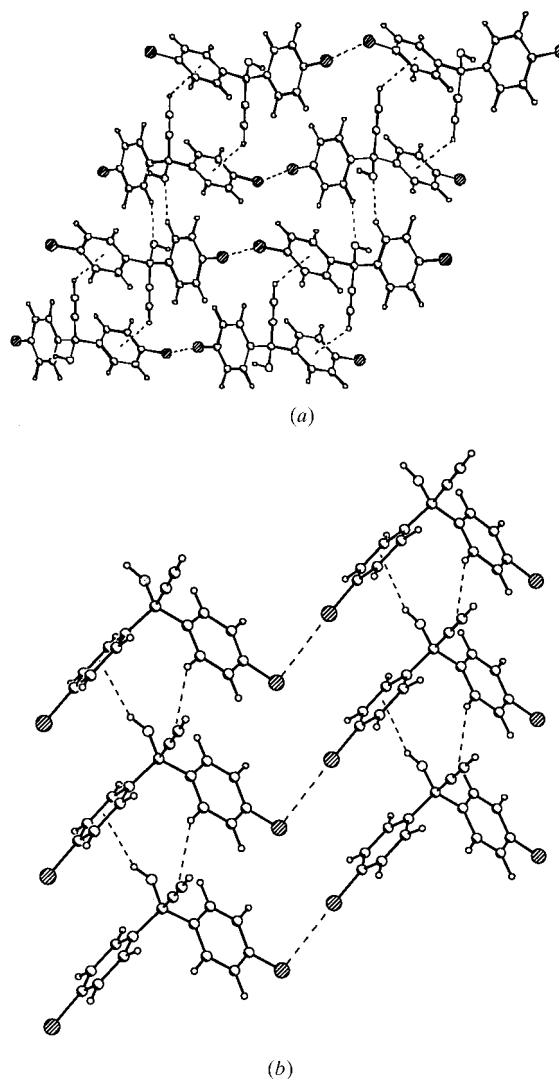


Figure 3
Perspective views of structure (3), displaying synthons II and III and halogen \cdots halogen interactions.

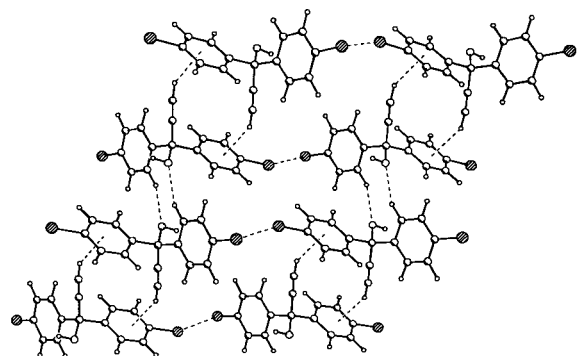
Table 1
Experimental details.

	(2)	(3) X-ray	(3) Neutron	(4)	(5)
Crystal data					
Chemical formula	C ₁₇ H ₁₆ O	C ₁₅ H ₁₀ Cl ₂ O	C ₁₅ H ₁₀ Cl ₂ O	C ₁₅ H ₁₀ Br ₂ O	C ₂₇ H ₂₀ O
Chemical formula weight	236.3	277.13	277.13	366.05	360.43
Cell setting	Triclinic	Triclinic	Triclinic	Triclinic	Triclinic
Space group	<i>P</i> $\bar{1}$	<i>P</i> $\bar{1}$	<i>P</i> $\bar{1}$	<i>P</i> $\bar{1}$	<i>P</i> $\bar{1}$
<i>a</i> (Å)	6.8286 (14)	5.7082 (1)	5.7280 (1)	5.7906 (12)	5.6413 (3)
<i>b</i> (Å)	8.2407 (16)	11.3645 (2)	11.3620 (2)	11.325 (2)	10.2599 (5)
<i>c</i> (Å)	12.658 (3)	11.5167 (1)	11.5210 (1)	11.907 (2)	17.3238 (9)
α (°)	106.73 (3)	117.268 (1)	117.240 (1)	115.67 (3)	100.450 (2)
β (°)	98.71 (3)	99.257 (1)	99.250 (1)	99.43 (3)	97.790 (2)
γ (°)	101.39 (3)	96.726 (1)	96.860 (1)	97.91 (3)	95.477 (2)
<i>V</i> (Å ³)	652.0 (2)	639.734 (17)	641.865 (17)	674.8 (2)	969.51 (9)
<i>Z</i>	2	2	2	2	2
<i>D_x</i> (Mg m ⁻³)	1.204	1.439	1.433	1.801	1.235
Radiation type	Mo <i>K</i> α	Mo <i>K</i> α	Neutron	Mo <i>K</i> α	Mo <i>K</i> α
Wavelength (Å)	0.71073	0.71073	–	0.71073	0.71073
No. of reflections for cell parameters	512	500	25	998	927
θ range (°)	5.33–29.35	5.44–29.17	–	4.26–30.50	10.15–26.52
μ (mm ⁻¹)	0.073	0.490	–	5.990	0.073
Temperature (K)	150	150	150	150	150
Crystal form	Block	Block	Block	Block	Plate
Crystal size (mm)	0.3 × 0.3 × 0.2	0.5 × 0.4 × 0.4	2.5 × 1.5 × 1.0	0.4 × 0.3 × 0.2	0.4 × 0.25 × 0.1
Crystal colour	Colourless	Colourless	Colourless	Colourless	Colourless
Data collection					
Diffractometer	Bruker SMART CCD	Bruker SMART CCD	SXD	Bruker SMART CCD	Bruker SMART CCD
Data collection method	ω scans	ω scans	Time-of-flight LAUE diffraction	ω scans	ω scans
Absorption correction	Multi-scan	Multi-scan	Empirical	Empirical	Empirical
<i>T</i> _{min}	0.784	0.284	0.51	0.344	0.681
<i>T</i> _{max}	1.000	0.332	0.89	0.766	0.884
No. of measured reflections	4775	4371	10 674	5364	12 424
No. of independent reflections	2964	2826	2929	3456	5270
No. of observed reflections	2362	2617	2928	2879	3419
Criterion for observed reflections	<i>I</i> > 2 σ (<i>I</i>)	<i>I</i> > 2 σ (<i>I</i>)	<i>I</i> > 2 σ (<i>I</i>)	<i>I</i> > 2 σ (<i>I</i>)	<i>I</i> > 2 σ (<i>I</i>)
<i>R</i> _{int}	0.0176	0.0425	0.062	0.0287	0.0426
θ _{max} (°)	27.48	27.31	16.16	30.16	30.45
Range of <i>h, k, l</i>	–8 → <i>h</i> → 8 –10 → <i>k</i> → 7 –14 → <i>l</i> → 16	–6 → <i>h</i> → 7 –11 → <i>k</i> → 14 –14 → <i>l</i> → 12	0 → <i>h</i> → 12 –20 → <i>k</i> → 21 –19 → <i>l</i> → 10	–6 → <i>h</i> → 8 –15 → <i>k</i> → 12 –15 → <i>l</i> → 16	–7 → <i>h</i> → 7 –14 → <i>k</i> → 13 –21 → <i>l</i> → 23
Refinement					
Refinement on	<i>F</i> ²	<i>F</i> ²	<i>F</i> ²	<i>F</i> ²	<i>F</i> ²
<i>R</i> [<i>F</i> ² > 2 σ (<i>F</i> ²)]	0.0478	0.0378	0.0668	0.0276	0.0759
<i>wR</i> (<i>F</i> ²)	0.1317	0.1043	0.1281	0.0718	0.2336
<i>S</i>	1.033	1.110	5.444	1.071	1.038
No. of reflections used in refinement	2964	2826	2929	3456	5270
No. of parameters used	231	203	253	203	322
H-atom treatment	All H-atom parameters refined	Mixed	All H-atom parameters refined	All H-atom parameters refined	All H-atom parameters refined
Weighting scheme	$w = 1/[\sigma^2(F_o^2) + (0.0618P)^2 + 0.2678P]$, where $P = (F_o^2 + 2F_c^2)/3$	$w = 1/[\sigma^2(F_o^2) + (0.0467P)^2 + 0.3533P]$, where $P = (F_o^2 + 2F_c^2)/3$	$w = 1/[\sigma^2(F_o^2)]$	$w = 1/[\sigma^2(F_o^2) + (0.0393P)^2 + 0.1818P]$, where $P = (F_o^2 + 2F_c^2)/3$	$w = 1/[\sigma^2(F_o^2) + (0.1193P)^2 + 0.5780P]$, where $P = (F_o^2 + 2F_c^2)/3$
(Δ/σ) _{max}	0.028	0.000	0.000	0.001	0.000
$\Delta\rho$ _{max} (e Å ⁻³)	0.205	0.332	0	0.862	0.503
$\Delta\rho$ _{min} (e Å ⁻³)	–0.197	–0.354	0	–0.433	–0.433
Extinction method	None	None	Becker–Coppens Lorentzian model	None	None
Extinction coefficient	–	–	0.296	–	–
Source of atomic scattering factors	<i>International Tables for Crystallography</i> (1992, Vol. C, Tables 4.2.6.8 and 6.1.1.4)	<i>International Tables for Crystallography</i> (1992, Vol. C, Tables 4.2.6.8 and 6.1.1.4)	<i>International Tables for Crystallography</i> (1992, Vol. C, Tables 4.4.4.1)	<i>International Tables for Crystallography</i> (1992, Vol. C, Tables 4.2.6.8 and 6.1.1.4)	<i>International Tables for Crystallography</i> (1992, Vol. C, Tables 4.2.6.8 and 6.1.1.4)

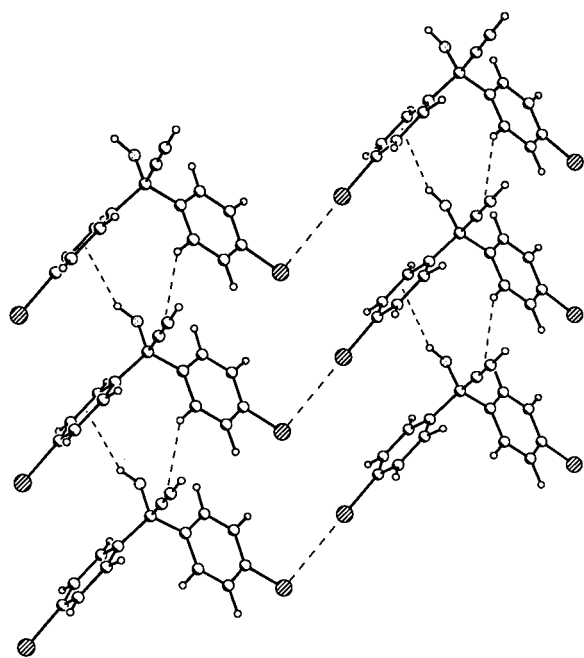
Table 1 (continued)

	(2)	(3) X-ray	(3) Neutron	(4)	(5)
Computer programs					
Data collection	SMART (Bruker Systems Inc., 1999a)	SMART (Bruker Systems Inc., 1999a)	SXD (Keen & Wilson, 1996)	SMART (Bruker Systems Inc., 1999a)	SMART (Bruker Systems Inc., 1999a)
Cell refinement	SMART (Bruker Systems Inc., 1999a)	SMART (Bruker Systems Inc., 1999a)	SXD (Keen & Wilson, 1996)	SMART (Bruker Systems Inc., 1999a)	SMART (Bruker Systems Inc., 1999a)
Data reduction	SAINT (Bruker Systems Inc., 1999b)	SAINT (Bruker Systems Inc., 1999b)	SXD (Keen & Wilson, 1996)	SAINT (Bruker Systems Inc., 1999b)	SAINT (Bruker Systems Inc., 1999b)
Structure solution	SHELXS97 (Sheldrick, 1997)	SHELXS97 (Sheldrick, 1997)	SHELXS97 (Sheldrick, 1997)	SHELXS97 (Sheldrick, 1997)	SHELXS97 (Sheldrick, 1997)
Structure refinement	SHELXL97 (Sheldrick, 1997)	SHELXL97 (Sheldrick, 1997)	SHELXL97 (Sheldrick, 1997)	SHELXL97 (Sheldrick, 1997)	SHELXL97 (Sheldrick, 1997)
Preparation of material for publication	SHELXL97 (Sheldrick, 1997)	SHELXL97 (Sheldrick, 1997)	SHELXL97 (Sheldrick, 1997)	SHELXL97 (Sheldrick, 1997)	SHELXL97 (Sheldrick, 1997)

of the halogen along the C–halogen bond vector, and δ^- perpendicular to the bond vector. Thus, an electrostatic C1–Cl1 \cdots Cl2–C2 interaction would be predicted to have $\theta_1 =$



(a)

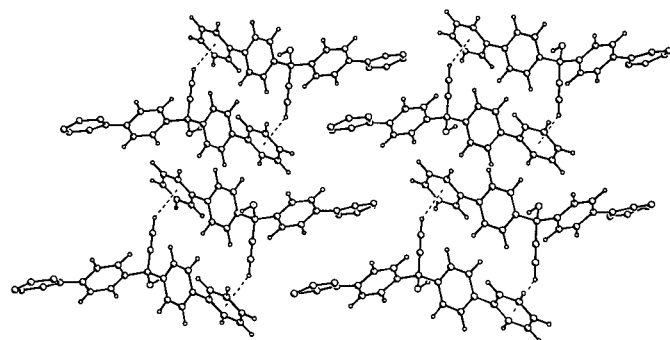


(b)

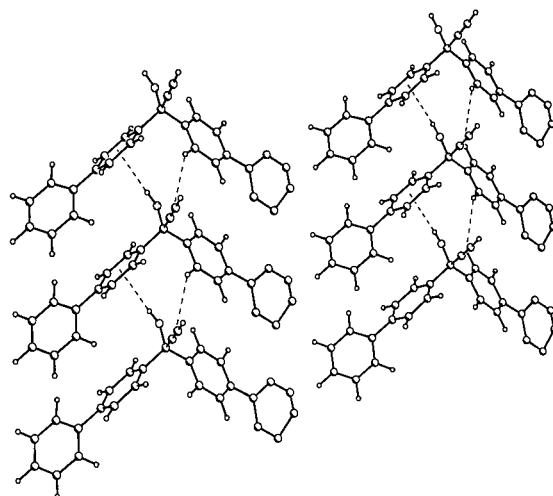
Figure 4

Perspective views of structure (4), displaying synthons II and III and halogen \cdots halogen interactions.

$\text{C1–Cl1}\cdots\text{Cl2} = 180^\circ$ and $\theta_2 = \text{Cl1}\cdots\text{Cl2–C2} = 90^\circ$. This is in accord with the type II interactions identified in crystal structures by Desiraju & Parthasarathy (1989) and Pedireddi *et al.* (1994) from a CSD analysis; their type I interactions ($\theta_1 = \theta_2$) arising from Cl \cdots Cl contacts across an inversion centre. The halogen \cdots halogen interactions observed in (3) and (4) (Table 3) have almost perfect type II geometry, with the Cl \cdots Cl and Br \cdots Br distances shorter than the appropriate van der Waals limits by 0.12 and 0.20 Å, respectively. The



(a)



(b)

Figure 5

Perspective views of structure (5), displaying synthons II and III.

Table 2
Fractional atomic coordinates and equivalent isotropic displacement parameters (\AA^2).

$$U_{\text{eq}} = (1/3)\sum_i \sum_j U^{ij} a^i a^j \mathbf{a}_i \cdot \mathbf{a}_j.$$

	<i>x</i>	<i>y</i>	<i>z</i>	U_{eq}
(2)				
O1	0.36138 (16)	0.14659 (15)	0.16398 (10)	0.0278 (3)
C1	0.7141 (3)	−0.0109 (2)	0.29487 (14)	0.0344 (4)
C2	0.6603 (2)	0.09261 (19)	0.25638 (13)	0.0266 (3)
C3	0.5790 (2)	0.21385 (18)	0.20481 (12)	0.0229 (3)
C4	0.6155 (2)	0.39365 (18)	0.29666 (12)	0.0224 (3)
C5	0.4550 (2)	0.4686 (2)	0.31962 (14)	0.0277 (3)
C6	0.4927 (3)	0.6303 (2)	0.40489 (14)	0.0303 (4)
C7	0.6903 (2)	0.71997 (19)	0.46824 (12)	0.0263 (3)
C8	0.7306 (3)	0.8924 (2)	0.56227 (15)	0.0356 (4)
C9	0.8508 (2)	0.6444 (2)	0.44306 (13)	0.0281 (3)
C10	0.8142 (2)	0.4830 (2)	0.35843 (13)	0.0272 (3)
C11	0.6815 (2)	0.23500 (17)	0.10758 (12)	0.0222 (3)
C12	0.5842 (2)	0.29838 (19)	0.02815 (13)	0.0260 (3)
C13	0.6724 (3)	0.3212 (2)	−0.06040 (13)	0.0282 (3)
C14	0.8597 (2)	0.28299 (18)	−0.07268 (13)	0.0266 (3)
C15	0.9529 (3)	0.3045 (2)	−0.17029 (15)	0.0362 (4)
C16	0.9569 (2)	0.22143 (19)	0.00761 (13)	0.0266 (3)
C17	0.8691 (2)	0.19732 (19)	0.09667 (13)	0.0248 (3)
(3) X-ray				
O1	1.1132 (2)	0.31881 (11)	0.44629 (13)	0.0267 (3)
C1	1.0066 (3)	−0.02664 (17)	0.30273 (19)	0.0305 (4)
C2	0.9579 (3)	0.08150 (16)	0.35028 (16)	0.0235 (3)
C3	0.9001 (3)	0.21751 (15)	0.40912 (16)	0.0214 (3)
C4	0.8200 (3)	0.24719 (14)	0.53893 (15)	0.0201 (3)
C5	0.9651 (3)	0.34161 (15)	0.66530 (16)	0.0243 (3)
C6	0.8855 (3)	0.36662 (16)	0.78075 (17)	0.0270 (3)
C7	0.6591 (3)	0.29600 (16)	0.76799 (16)	0.0249 (3)
C11	0.04963 (8)	0.26483 (5)	0.05839 (5)	0.03706 (14)
C8	0.5132 (3)	0.20033 (17)	0.64306 (17)	0.0272 (3)
C9	0.5949 (3)	0.17631 (17)	0.52931 (16)	0.0252 (3)
C10	0.6949 (3)	0.22598 (15)	0.31106 (15)	0.0214 (3)
C11	0.6523 (3)	0.35366 (15)	0.33946 (17)	0.0253 (3)
C12	0.4577 (3)	0.36638 (17)	0.26036 (17)	0.0276 (3)
C13	0.3042 (3)	0.25021 (17)	0.15251 (16)	0.0271 (3)
C12	0.55431 (8)	0.32701 (5)	0.91110 (4)	0.03824 (15)
C14	0.3448 (3)	0.12307 (17)	0.12157 (17)	0.0291 (3)
C15	0.5417 (3)	0.11124 (16)	0.20127 (17)	0.0264 (3)
(3) Neutron				
O1	1.1102 (4)	0.3181 (2)	0.4452 (3)	0.0268 (5)
C11	0.0542 (3)	0.26511 (16)	0.05897 (17)	0.0421 (4)
C1	1.0047 (4)	−0.02661 (18)	0.3033 (2)	0.0333 (5)
C2	0.9559 (3)	0.08311 (16)	0.35113 (19)	0.0223 (4)
C3	0.8984 (3)	0.21786 (15)	0.40894 (17)	0.0187 (3)
C4	0.8194 (3)	0.24703 (14)	0.53838 (16)	0.0171 (3)
C5	0.9649 (3)	0.34106 (16)	0.66423 (18)	0.0236 (4)
C6	0.8860 (4)	0.36646 (17)	0.78000 (19)	0.0269 (4)
C7	0.6603 (3)	0.29618 (17)	0.76792 (18)	0.0236 (4)
C8	0.5148 (4)	0.2012 (2)	0.6435 (2)	0.0278 (4)
C9	0.5950 (3)	0.17659 (18)	0.52866 (19)	0.0247 (4)
C10	0.6940 (3)	0.22635 (15)	0.31199 (17)	0.0193 (3)
C11	0.6513 (4)	0.35329 (16)	0.34004 (19)	0.0248 (4)
C12	0.4579 (4)	0.36662 (18)	0.2611 (2)	0.0282 (4)
C13	0.3053 (4)	0.25032 (18)	0.15295 (19)	0.0266 (4)
C12	0.5579 (3)	0.32699 (17)	0.91032 (17)	0.0434 (4)
C14	0.3467 (4)	0.12323 (18)	0.1226 (2)	0.0299 (4)
C15	0.5422 (4)	0.11157 (17)	0.20187 (19)	0.0265 (4)
(4)				
O1	0.3788 (3)	0.17949 (17)	1.05754 (17)	0.0280 (3)
Br1	1.45503 (4)	0.23580 (3)	1.44526 (2)	0.03392 (8)
Br2	0.95564 (5)	0.17469 (3)	0.60197 (2)	0.03739 (8)
C1	0.4884 (4)	0.5239 (3)	1.1907 (3)	0.0314 (5)
C2	0.5352 (4)	0.4170 (2)	1.1473 (2)	0.0243 (4)
C3	0.5921 (4)	0.2826 (2)	1.0935 (2)	0.0222 (4)

Table 2 (continued)

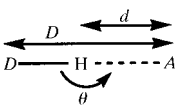
	<i>x</i>	<i>y</i>	<i>z</i>	U_{eq}
C4	0.7950 (4)	0.2749 (2)	1.1894 (2)	0.0220 (4)
C5	0.9410 (4)	0.3879 (2)	1.2966 (2)	0.0283 (5)
C6	1.1362 (4)	0.3768 (2)	1.3750 (2)	0.0297 (5)
C7	1.1801 (4)	0.2507 (2)	1.3444 (2)	0.0261 (4)
C8	1.0325 (4)	0.1356 (2)	1.2387 (2)	0.0274 (4)
C9	0.8406 (4)	0.1481 (2)	1.1613 (2)	0.0263 (4)
C10	0.6726 (4)	0.2554 (2)	0.9690 (2)	0.0208 (4)
C11	0.5266 (4)	0.1636 (2)	0.8476 (2)	0.0242 (4)
C12	0.6082 (4)	0.1394 (2)	0.7376 (2)	0.0260 (4)
C13	0.8365 (4)	0.2090 (2)	0.7505 (2)	0.0247 (4)
C14	0.9833 (4)	0.3029 (2)	0.8698 (2)	0.0263 (4)
C15	0.8996 (4)	0.3258 (2)	0.9790 (2)	0.0250 (4)
(5)				
O1	0.0883 (3)	0.26591 (16)	0.32794 (10)	0.0326 (4)
C1	0.0423 (4)	−0.0743 (3)	0.29797 (15)	0.0354 (5)
C2	0.1443 (4)	0.0348 (2)	0.30668 (13)	0.0297 (5)
C3	0.2633 (4)	0.1735 (2)	0.31647 (13)	0.0277 (4)
C4	0.3638 (4)	0.1901 (2)	0.24024 (13)	0.0275 (4)
C5	0.2812 (6)	0.2778 (3)	0.19456 (17)	0.0510 (8)
C6	0.3804 (7)	0.2913 (4)	0.12649 (19)	0.0662 (10)
C7	0.5632 (4)	0.2191 (2)	0.10295 (15)	0.0387 (5)
C8	0.6933 (12)	0.2569 (7)	0.0337 (4)	0.0444 (16)
C8A	0.6508 (10)	0.2181 (6)	0.0279 (3)	0.0345 (13)
C9	0.7488 (13)	0.1532 (8)	−0.0184 (4)	0.0479 (17)
C9A	0.8893 (16)	0.1860 (9)	0.0183 (5)	0.0309 (18)
C9B	0.755 (2)	0.1131 (15)	−0.0142 (9)	0.047 (3)
C10	0.9392 (17)	0.3032 (10)	−0.0909 (6)	0.079 (2)
C10A	0.984 (2)	0.1971 (11)	−0.0516 (7)	0.045 (2)
C10B	0.8428 (18)	0.1373 (12)	−0.0838 (6)	0.032 (2)
C11	0.8695 (17)	0.1854 (10)	−0.0857 (6)	0.070 (2)
C11A	0.776 (3)	0.2539 (14)	−0.1172 (8)	0.051 (4)
C11B	0.857 (2)	0.2489 (10)	−0.1105 (6)	0.0241 (19)
C12	0.9046 (16)	0.4169 (8)	−0.0341 (5)	0.076 (2)
C12A	0.595 (2)	0.2654 (12)	−0.1054 (7)	0.051 (3)
C12B	0.758 (2)	0.3675 (13)	−0.0672 (8)	0.054 (3)
C13	0.7765 (13)	0.3910 (7)	0.0277 (4)	0.0614 (16)
C13A	0.5090 (19)	0.2510 (11)	−0.0363 (7)	0.042 (2)
C13B	0.654 (2)	0.3512 (11)	−0.0001 (7)	0.044 (2)
C14	0.6400 (5)	0.1299 (3)	0.14867 (16)	0.0410 (6)
C15	0.5424 (5)	0.1155 (3)	0.21671 (17)	0.0418 (6)
C16	0.4697 (4)	0.2080 (2)	0.38763 (13)	0.0265 (4)
C17	0.5842 (4)	0.1103 (2)	0.41913 (14)	0.0302 (5)
C18	0.7747 (4)	0.1467 (2)	0.48245 (14)	0.0291 (5)
C19	0.8535 (3)	0.2812 (2)	0.51612 (12)	0.0248 (4)
C20	1.0514 (3)	0.3190 (2)	0.58493 (12)	0.0247 (4)
C21	1.2571 (4)	0.2522 (2)	0.58795 (14)	0.0287 (5)
C22	1.4380 (4)	0.2851 (2)	0.65346 (15)	0.0342 (5)
C23	1.4181 (5)	0.3860 (3)	0.71682 (16)	0.0414 (6)
C24	1.2180 (4)	0.4552 (3)	0.71411 (15)	0.0385 (6)
C25	1.0358 (4)	0.4217 (2)	0.64876 (14)	0.0299 (5)
C26	0.7358 (4)	0.3784 (2)	0.48418 (13)	0.0262 (4)
C27	0.5500 (4)	0.3425 (2)	0.42013 (13)	0.0272 (4)

more significant interpenetration of the Br spheres is suggested by both the theoretical and database analyses cited above and reflects the increased polarizability of Br.

3.4. Bis(4,4'-biphenyl)ethynylmethanol (5)

The structure of (5), in which one of the substituent phenyl rings is disordered over three positions with relative site occupancies in the ratio 2:1:1, is very similar to those of (3) and (4). Inversion-related molecules form dimers through a pair of $\text{C}\equiv\text{C}-\text{H}\cdots\pi(\text{arene})$ bonds (Fig. 5a) to the ordered phenyl substituent. The synthon thus formed is a variant of synthon II

Table 3
Intermolecular interaction geometries.



		Experimental			H-normalized	
		D (Å)	d (Å)	θ (°)	d (Å)	θ (°)
(2)	O—H...X1†‡	3.324	2.484	167.9	2.358	167.2
	C≡C—H...X1†‡	3.987	3.137	149.5	3.025	148.2
	C—H...O	3.705 (2)	2.90 (3)	139 (2)	2.831	138
	C—H...X1†‡	3.525	2.768	138.4	2.662	136.3
(3) X-ray	C—H...X2†§	3.794	2.996	139.0	2.922	137.8
	O—H...X1†‡	3.463	2.743	157.4	2.544	155.52
	C≡C—H...X1†‡	3.472	2.722	138.8	2.608	136.2
	C—H...O	3.330 (2)	2.47 (2)	152 (1)	2.341	151
	C—H...X2§	3.776	2.858	157.6	2.756	156.7
(3) Neutron	Cl...Cl		3.375 (6)	172.96 (6), 93.54 (5)		
	O—H...X1†‡	3.471	2.569	158.43		
	C≡C—H...X1†‡	3.481	2.637	137.7		
	C—H...O	3.341 (3)	2.361 (4)	150.2 (3)		
(4)	C—H...X2§	3.781	2.759	157.1		
	Cl...Cl		3.394 (2)	173.0 (1), 93.85 (9)		
	O—H...X1†‡	3.560	2.835	159.2	2.633	157.5
	C≡C—H...X1†‡	3.483	2.684	148.1	2.532	145.9
	C—H...O	3.378 (3)	2.56 (3)	157 (2)	2.37	155
(5)	C—H...X2§	3.840	2.970	156.0	2.833	154.7
	Br...Br		3.502 (1)	173.79 (7), 93.42 (7)		
	O—H...X1†‡	3.451	2.630	157.0	2.530	156.0
	C≡C—H...X1†‡	3.446	2.641	151.8	2.468	149.6

† Distances and angles measured to the mid-point of the triple bond and aromatic ring. ‡ X1 is the centroid of an aromatic ring. § X2 is the centroid of the triple bond.

(Fig. 6) in which, by comparison with the occurrence of this synthon in (3) and (4), there is an intervening phenyl ring. Molecules related by an a translation are linked by O—H... π (arene) interactions (synthon III, Fig. 6) in exactly the same way as the a -translated molecules in (3) and (4) (*cf.* Fig. 5*b* with Figs. 3*b* and 4*b*), leading to the close similarity in the a cell dimensions in all three structures (Table 1).

Molecular packing along the c axis is mediated by herringbone interactions between ordered and disordered peripheral phenyl rings. These interactions substitute for the type II halogen...halogen interactions in (3) and (4), a factor reinforced by the similar (perpendicular) topologies of the two interaction types. Thus, the overall packing arrangement of (5), as depicted in Figs. 5(*a*) and (*b*), bears a striking resemblance to the arrangements in (3) and (4) (Figs. 3*a*, *b*, 4*a* and *b*). Note that the disordered phenyl ring is involved in the looser herringbone interactions, while the ring involved in synthon II is ordered, thus indicating the relative strength of the C≡C—H... π (arene) interaction.

3.5. Neutron study of di(4-chlorophenyl)ethynylmethanol (3)

The importance of neutron diffraction results to the accurate study of hydrogen-bond geometries is unquestionable. This is especially true (*a*) where the chemical nature of the donor group makes it difficult to estimate true H-atom positions with any degree of certainty, *e.g.* in the case of O—H donors, and (*b*) in the study of hydrogen bonds to diffuse

acceptor density, *e.g.* the π -density of arene rings or ethynyl bonds. Both of these situations occur in structure (3).

The neutron-derived geometry for the O—H... π (arene), C≡C—H... π (arene), C—H...O and C(phenyl)—H... π (ethynyl) interactions is given in Table 3. It is clear that the relevant C—H donor vectors are not collinear with the centres of arene or ethynyl π -density and this is not unexpected. A combination of IR spectroscopic studies (Steiner *et al.*, 1996) and neutron diffraction data (Steiner *et al.*, 1997) have shown that off-centre O—H... π (arene) interactions do indeed exhibit hydrogen-bond characteristics, while gas-phase studies (Suzuki *et al.*, 1992) have shown that the acceptor directionality of aromatic rings is extremely soft, allowing for a wide range of geometries to exist that have closely similar

interaction energies. We note that the directionality at H in the X—H interactions with π -systems in (3) is at least as good, *i.e.* as close to linear, as it is in the C—H...O interaction.

The single-structure observations in (3) are fully corroborated by an examination of the relevant scatterplots in *IsoStar* (Bruno *et al.*, 1997), the knowledge base of intermolecular

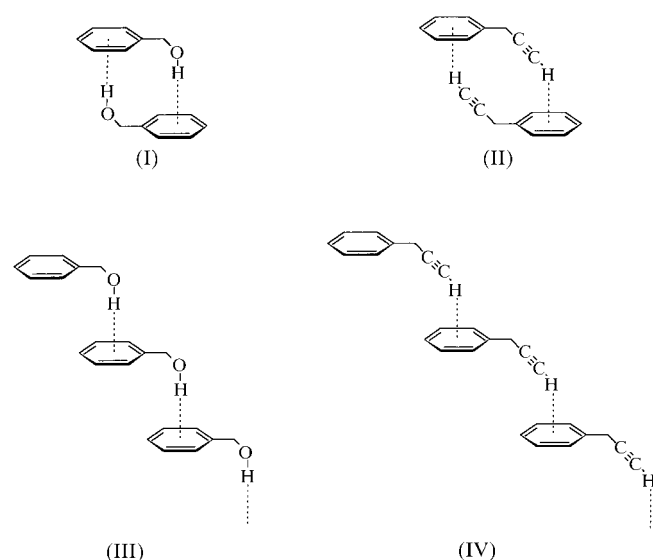


Figure 6
Synthons I, II, III and IV.

interactions derived from the CSD, and distributed as part of CSD system releases. Fig. 7 shows (static) scatterplots of the approach of C–H contact groups to (a) phenyl rings, and (b) and (c) ethynyl groups. These plots are derived primarily from X-ray data, the dominant experimental source in the CSD, but with X-ray determined H-atom positions normalized so that their C–H distance reflects the mean value obtained in neutron experiments, but with the X-ray determined C–H vector direction unchanged. In Table 3, we also compare the

neutron-derived hydrogen-bond geometries in (3) with those from the low-temperature X-ray study in which the H-atom positions have been normalized in this way. The hydrogen-bond distances and hydrogen-bond directionalities at H derived from the normalized X-ray data are reassuringly close to those in the low-temperature neutron study. This provides some evidence, albeit from a single structure, of the value of the hydrogen-normalization procedure, now regarded as best practice in the analysis of hydrogen-bond geometries from X-ray data. Thus encouraged, we are now undertaking a more complete comparison of hydrogen-bond geometries determined by neutron diffraction with those derived from normalized X-ray data, using the CSD to identify suitable structures determined by both techniques.

3.6. Structural comparison of *gem*-alkynols (1)–(5)

The complete lack of the expected strong O–H···O hydrogen bonds in parent (1) is observed throughout the series (2)–(5) studied here. However, the OH group in *gem*-alkynols is already sterically hindered by the extended ethynyl moiety and this difficulty is accentuated by the presence of additional phenyl substituents at the *gem*-alkynol centre. Thus, rather than forming O–H···O bonds, the two most acidic protons, O–H and C≡C–H, participate in weak hydrogen bonds to π -acceptors, which stabilize all five structures through the formation of synthons I–IV of Fig. 6. These primary interactions are reinforced by a variety of other weak interactions involving C(ethynyl)–H, C(phenyl)–H and even C(methyl)–H as donors and the hydroxy-O as acceptor, together with halogen···halogen interactions in (3) and (4).

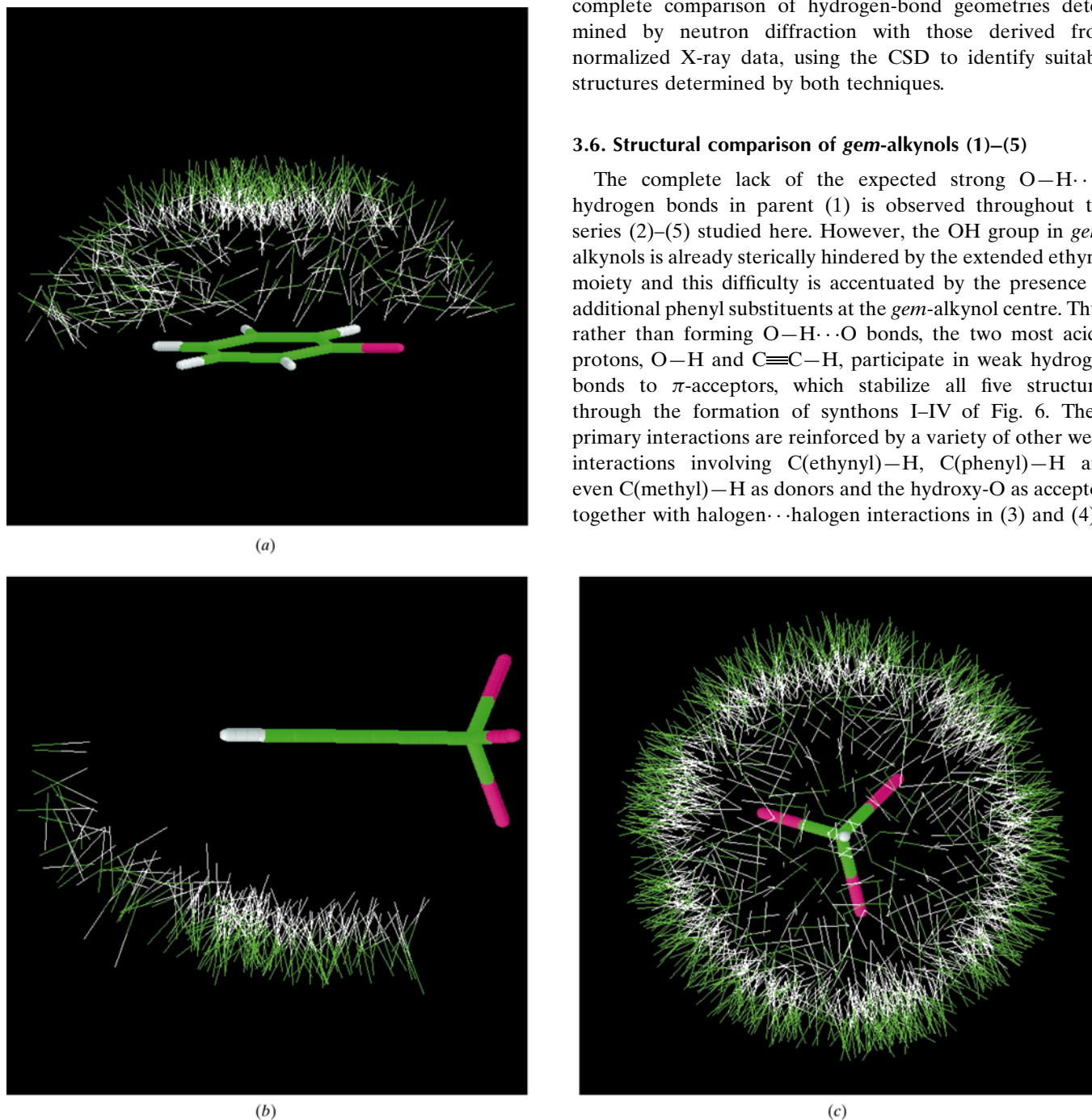


Figure 7

Scatterplots from *IsoStar* (Bruno *et al.*, 1997) showing the approach of alkyl C–H to (a) phenyl rings, and (b) and (c) to ethynyl groups. Part (b) views the interaction space along the $-\text{C}\equiv\text{C}-\text{H}$ vector, and (c) is a slice through this space viewed perpendicular to the $-\text{C}\equiv\text{C}-\text{H}$ vector.

Comparison of the structures reveals interesting transitions along the series (1)–(5). Thus, in parent (1) the OH groups participate in the cyclic synthon I, while the ethynyl group takes part in a cooperative chain. The replacement of the *para*-H atoms by methyl groups retains synthon I in (2), but the ethynyl groups now participate in another π -directed synthon IV. In structures (3), (4) and (5), where the *para*-H are now replaced by halogen or phenyl substituents having their own capacity to form non-covalent interactions, the *gem*-alkynol functionality now participates in synthons II and III, albeit in an extended form of II in (5). The formation of different π -acceptor synthons in the different structures is clearly related to the interaction possibilities and requirements of the various substituents. Thus, although the dimethyl derivative (2) and the dichloro derivative (3) resemble each other in forming O–H $\cdots\pi$ (arene) and C \equiv C–H $\cdots\pi$ (arene) bonds, the synthons formed are very different (I *versus* II), and their overall structures are very different, owing to the interaction requirements of the methyl C–H against C–Cl. Although it has been observed (Desiraju & Sarma, 1986) that methyl/chloro interchange does not disrupt structures where these groups merely play a space-filling role, it seems clear that this cannot be the case when interactions involving these groups are intimately involved in structural organization.

While structures (1)–(5) do show a degree of synthon repetitiveness, synthon I being preserved in (1) and (2), and synthon II in structures (3), (4) and (5), this repetitiveness is not complete across the series. However, the topological similarity of synthons I and II is obvious, the former being mediated by O–H donors and the latter by C \equiv C–H. It is known (James *et al.*, 1996; Davis *et al.*, 1996) that hydroxy and ethynyl groups are capable of forming equivalent synthons when hydrogen-bonded to themselves. The present structures indicate that such an equivalence can also occur when these groups are involved in hydrogen bonds to other acceptors as weak as phenyl rings. The synthon similarity across the series (1)–(5), combined with the robustness of the synthons formed, points to their further application in crystal engineering.

The EPSRC (UK) are thanked for financial support to CB and JAKH (Senior Research Fellowship), and the CSIR (India) for financial support to NNLM. This work has been conducted under the Indo-UK bilateral cooperation project No. INT/UK/P-15/99 of the Department of Science and Technology, Government of India and the British Council.

References

- Allen, F. H., Hoy, V. J., Howard, J. A. K., Thalladi, V. R. & Desiraju, G. R. (1997). *J. Am. Chem. Soc.* **119**, 3477–3480.
 Allen, F. H. & Kennard, O. (1993). *Chem. Des. Autom. News*, **8**, 1, 31–37.

- Bilton, C., Howard, J. A. K., Madhavi, N. N. L., Nangia, A., Desiraju, G. R., Allen, F. H. & Wilson, C. C. (1999). *J. Chem. Soc. Chem. Commun.* pp. 1675–1676.
 Bruker Systems Inc. (1999a). *SMART*. Bruker Systems Inc., Madison, Wisconsin, USA.
 Bruker Systems Inc. (1999b). *SAINTE*. Bruker Systems Inc., Madison, Wisconsin, USA.
 Bruno, I. J., Cole, J. C., Lommerse, J. P. M., Rowland, R. S., Taylor, R. & Verdonk, M. L. (1997). *J. Comput.-Aided Mol. Des.* **11**, 525–537.
 Davis, P. L., Veldman, N., Grove, D. M., Spek, A. L., Lutz, B. T. G. & van Koten, G. (1996). *Angew. Chem. Int. Ed. Engl.* **35**, 1959–1961.
 Desiraju, G. R. (1995). *Angew. Chem. Int. Ed. Engl.* **34**, 2311–2327.
 Desiraju, G. R. (1997). *Chem. Commun.* pp. 1475–1476.
 Desiraju, G. R. & Parthasarathy, R. (1989). *J. Am. Chem. Soc.* **111**, 8725–8726.
 Desiraju, G. R. & Sarma, J. A. R. P. (1986). *Proc. Indian Acad. Sci. (Chem. Sci.)* **96**, 599–605.
 Desiraju, G. R. & Steiner, T. (1999). *The Weak Hydrogen Bond in Structural Chemistry and Biology*. Oxford University Press.
 Ermer, O. & Eling, A. (1994). *J. Chem. Soc. Perkin Trans. 2*, pp. 925–944.
 Etter, M. C. (1990). *Acc. Chem. Res.* **23**, 120–126.
 Ferguson, G., Gallagher, J. F., Glidewell, C. & Zakaria, C. M. (1994). *Acta Cryst.* **C50**, 70–73.
 Garcia, J. G., Ramos, B. & Rodriguez, A. (1995). *Acta Cryst.* **C51**, 2674–2676.
 Keen, D. A. & Wilson, C. C. (1996). Technical Report RAL-TR-96-083. *Single Crystal Diffraction at ISIS. User Guide for the SXD Instrument*. CCLRC Rutherford Appleton Laboratory, Chilton, England.
 James, S. L., Verspui, G., Spek, A. L. & van Koten, G. (1996). *Chem. Commun.* pp. 1309–1310.
 Lommerse, J. P. M., Stone, A. J., Taylor, R. & Allen, F. H. (1996). *J. Am. Chem. Soc.* **118**, 3108–3116.
 Lutz, B., Kanters, J. A., van der Maas, J., Kroon, J. & Steiner, T. (1998). *J. Mol. Struct.* pp. 81–87.
 Madhavi, N. N. L., Bilton, C., Howard, J. A. K., Allen, F. H., Nangia, A. & Desiraju, G. R. (2000). *New J. Chem.* **24**, 1–4.
 Madhavi, N. N. L., Desiraju, G. R., Bilton, C., Howard, J. A. K. & Allen, F. H. (2000). *Acta Cryst.* **B56**, 1063–1070.
 Nangia, A. & Desiraju, G. R. (1998). *Top. Curr. Chem.* **198**, 57–95.
 Nishio, M., Hirota, M. & Umezama, Y. (1998). *The CH π Interaction, Evidence, Nature and Consequences*. New York: Wiley.
 Pedireddi, V. R., Reddy, D. S., Goud, B. S., Craig, D. C., Rae, A. D. & Desiraju, G. R. (1994). *J. Chem. Soc. Perkin Trans. 2*, pp. 2353–2360.
 Pedireddi, V. R., Sarma, J. A. R. P. & Desiraju, G. R. (1992). *J. Chem. Soc. Perkin Trans. 2*, pp. 311–320.
 Price, S. L., Stone, A. J., Lucas, J., Rowland, R. S. & Thornley, A. E. (1994). *J. Am. Chem. Soc.* **116**, 4910–4918.
 Sheldrick, G. M. (1997). *SHELX97*. University of Göttingen, Germany.
 Steiner, T., Mason, S. A. & Tamm, M. (1997). *Acta Cryst.* **B53**, 843–848.
 Steiner, T., Starikov, E. B., Amado, A. M. & Teixeira-Dias, J. J. C. (1995). *J. Chem. Soc. Perkin Trans. 2*, pp. 1321–1326.
 Steiner, T., Starikov, E. B. & Tamm, M. (1996). *J. Chem. Soc. Perkin Trans. 2*, pp. 67–71.
 Steiner, T., Tamm, M., Lutz, B. & van der Maas, J. H. (1996). *Chem. Commun.* pp. 1127–1128.
 Steinwender, E., Lutz, E. T. G., van der Maas, J. H. & Kanters, J. A. (1993). *Vib. Spectrosc.* **4**, 217–229.
 Suzuki, S., Green, P. G., Bumgarner, R. E., Dasgupta, S., Goddard III, W. A. & Blake, G. A. (1992). *Science*, **257**, 942–944.
 Wilson, C. C. (1997). *J. Mol. Struct.* pp. 207–217.